

# Adaptive liquid crystal microlens array enabled by two-photon polymerization

ZIQIAN HE,<sup>1</sup> YUN-HAN LEE,<sup>1</sup> DEBASHIS CHANDA,<sup>1,2,3,4</sup> AND SHIN-TSON WU<sup>1,5</sup>

<sup>1</sup>College of Optics and Photonics, University of Central Florida, Orlando, FL 32816, USA

<sup>2</sup>Department of Physics, University of Central Florida, Orlando, FL 32816, USA

<sup>3</sup>NanoScience Technology Center, University of Central Florida, Orlando, FL 32826, USA

<sup>4</sup>Debashis.Chanda@creol.ucf.edu

<sup>5</sup>swu@creol.ucf.edu

**Abstract:** A tunable-focus liquid crystal microlens array is demonstrated and characterized. Using two-photon polymerization based direct-laser writing, a polymerized microlens array is fabricated on one substrate. Such a microlens array creates inhomogeneous electric field distribution and homogeneous-like liquid-crystal alignment, simultaneously. The phase profile and thus the focal length can be tuned dynamically by the applied voltage. We also further investigate the focusing property and the imaging capability of the fabricated sample. Using the adaptive microlens array as an example, we demonstrate that directly forming a curvilinear surface with liquid-crystal alignment is feasible. In addition to adaptive lens, this direct-laser writing method is also a powerful tool for making other tunable photonic devices.

© 2018 Optical Society of America under the terms of the [OSA Open Access Publishing Agreement](#)

**OCIS codes:** (230.3720) Liquid-crystal devices; (220.1140) Alignment; (110.2760) Gradient-index lenses; (220.4241) Nanostructure fabrication.

## References and links

1. T. Nose, S. Masuda, S. Sato, J. Li, L. C. Chien, and P. J. Bos, "Effects of low polymer content in a liquid-crystal microlens," *Opt. Lett.* **22**(6), 351–353 (1997).
2. A. F. Naumov, M. Yu. Loktev, I. R. Guralnik, and G. Vdovin, "Liquid-crystal adaptive lenses with modal control," *Opt. Lett.* **23**(13), 992–994 (1998).
3. Y. Choi, J.-H. Park, J.-H. Kim, and S.-D. Lee, "Fabrication of a focal length variable microlens array based on a nematic liquid crystal," *Opt. Mater.* **21**(1-3), 643–646 (2003).
4. H. Ren and S.-T. Wu, "Tunable electronic lens using a gradient polymer network liquid crystal," *Appl. Phys. Lett.* **82**(1), 22–24 (2003).
5. V. V. Presnyakov and T. V. Galstian, "Electrically tunable polymer stabilized liquid-crystal lens," *J. Appl. Phys.* **97**(10), 103101 (2005).
6. Y. H. Lin, H. S. Chen, H. C. Lin, Y. S. Tsou, H. K. Hsu, and W. Y. Li, "Polarizer-free and fast response microlens arrays using polymer-stabilized blue phase liquid crystals," *Appl. Phys. Lett.* **96**(11), 113505 (2010).
7. Y. Y. Kao, P. C. P. Chao, and C. W. Hsueh, "A new low-voltage-driven GRIN liquid crystal lens with multiple ring electrodes in unequal widths," *Opt. Express* **18**(18), 18506–18518 (2010).
8. L. Lu, V. Sergan, T. Van Heugten, D. Duston, A. Bhowmik, and P. J. Bos, "Surface localized polymer aligned liquid crystal lens," *Opt. Express* **21**(6), 7133–7138 (2013).
9. A. Orth and K. Crozier, "Microscopy with microlens arrays: high throughput, high resolution and light-field imaging," *Opt. Express* **20**(12), 13522–13531 (2012).
10. Y. H. Lin, Y. J. Wang, and V. Reshetnyak, "Liquid crystal lenses with tunable focal length," *Liq. Cryst. Rev.* **5**(2), 111–143 (2017).
11. P.-Y. Hsieh, P.-Y. Chou, H.-A. Lin, C.-Y. Chu, C.-T. Huang, C.-H. Chen, Z. Qin, M. M. Corral, B. Javidi, and Y.-P. Huang, "Long working range light field microscope with fast scanning multifocal liquid crystal microlens array," *Opt. Express* **26**(8), 10981–10996 (2018).
12. J. F. Algorri, N. Bennis, V. Urruchi, P. Morawiak, J. M. Sánchez-Pena, and L. R. Jaroszewicz, "Tunable liquid crystal multifocal microlens array," *Sci. Rep.* **7**(1), 17318 (2017).
13. S. Masuda, S. Takahashi, T. Nose, S. Sato, and H. Ito, "Liquid-crystal microlens with a beam-steering function," *Appl. Opt.* **36**(20), 4772–4778 (1997).
14. J. Sun, S. Xu, H. Ren, and S.-T. Wu, "Reconfigurable fabrication of scattering-free polymer network liquid crystal prism/grating/lens," *Appl. Phys. Lett.* **102**(16), 161106 (2013).
15. A. Akatay, C. Ataman, and H. Urey, "High-resolution beam steering using microlens arrays," *Opt. Lett.* **31**(19), 2861–2863 (2006).

16. L. Hu, L. Xuan, D. Li, Z. Cao, Q. Mu, Y. Liu, Z. Peng, and X. Lu, "Wavefront correction based on a reflective liquid crystal wavefront sensor," *J. Opt. A, Pure Appl. Opt.* **11**(1), 015511 (2009).
17. J.-H. Na, S.-C. Park, S.-U. Kim, Y. Choi, and S.-D. Lee, "Physical mechanism for flat-to-lenticular lens conversion in homogeneous liquid crystal cell with periodically undulated electrode," *Opt. Express* **20**(2), 864–869 (2012).
18. C. W. Chen, Y. P. Huang, and P. C. Chen, "Dual direction overdriving method for accelerating 2D/3D switching time of liquid crystal lens on auto-stereoscopic display," *J. Disp. Technol.* **8**(10), 559–561 (2012).
19. X. Wang, Y. Qin, H. Hua, Y. H. Lee, and S. T. Wu, "Digitally switchable multi-focal lens using freeform optics," *Opt. Express* **26**(8), 11007–11017 (2018).
20. M. C. Tseng, F. Fan, C. Y. Lee, A. Murauski, V. Chigrinov, and H. S. Kwok, "Tunable lens by spatially varying liquid crystal pretilt angles," *J. Appl. Phys.* **109**(8), 083109 (2011).
21. V. S. Bezruchenko, A. A. Muravsky, A. A. Murauski, A. I. Stankevich, and U. V. Mahilny, "Tunable liquid crystal lens based on pretilt angle gradient alignment," *Mol. Cryst. Liq. Cryst. (Phila. Pa.)* **626**(1), 222–228 (2016).
22. Y.-H. Fan, H. Ren, X. Liang, H. Wang, and S.-T. Wu, "Liquid crystal microlens arrays with switchable positive and negative focal lengths," *J. Disp. Technol.* **1**(1), 151–156 (2005).
23. M. Ye and S. Sato, "Optical properties of liquid crystal lens of any size," *Jpn. J. Appl. Phys.* **41**(41), 571–573 (2002).
24. H. Ren, Y.-H. Fan, S. Gauza, and S.-T. Wu, "Tunable microlens arrays using polymer network liquid crystal," *Opt. Commun.* **230**(4-6), 267–271 (2004).
25. K. Asatryan, V. Presnyakov, A. Tork, A. Zohrabyan, A. Bagramyan, and T. Galstian, "Optical lens with electrically variable focus using an optically hidden dielectric structure," *Opt. Express* **18**(13), 13981–13992 (2010).
26. L. G. Commander, S. E. Day, and D. R. Selviah, "Variable focal length microlenses," *Opt. Commun.* **177**(1-6), 157–170 (2000).
27. M. Schadt, K. Schmitt, V. Kozinkov, and V. Chigrinov, "Surface-induced parallel alignment of liquid crystals by linearly polymerized photopolymers," *Jpn. J. Appl. Phys.* **31**(7), 2155–2164 (1992).
28. B. H. Cumpston, S. P. Ananthavel, S. Barlow, D. L. Dyer, J. E. Ehrlich, L. L. Erskine, A. A. Heikal, S. M. Kuebler, I.-Y. S. Lee, D. McCord-Maughon, J. Qin, H. Röckel, M. Rumi, X. L. Wu, S. R. Marder, and J. W. Perry, "Two-photon polymerization initiators for three-dimensional optical data storage and microfabrication," *Nature* **398**(6722), 51–54 (1999).
29. J. Serbin, A. Egbert, A. Ostendorf, B. N. Chichkov, R. Houbertz, G. Domann, J. Schulz, C. Cronauer, L. Fröhlich, and M. Popall, "Femtosecond laser-induced two-photon polymerization of inorganic-organic hybrid materials for applications in photonics," *Opt. Lett.* **28**(5), 301–303 (2003).
30. Y.-H. Lee, D. Franklin, F. Gou, G. Liu, F. Peng, D. Chanda, and S.-T. Wu, "Two-photon polymerization enabled multi-layer liquid crystal phase modulator," *Sci. Rep.* **7**(1), 16260 (2017).
31. D. Franklin, Y. Chen, A. Vazquez-Guardado, S. Modak, J. Boroumand, D. Xu, S.-T. Wu, and D. Chanda, "Polarization-independent actively tunable colour generation on imprinted plasmonic surfaces," *Nat. Commun.* **6**(1), 7337 (2015).
32. Z. He, Y.-H. Lee, F. Gou, D. Franklin, D. Chanda, and S.-T. Wu, "Polarization-independent phase modulators enabled by two-photon polymerization," *Opt. Express* **25**(26), 33688–33694 (2017).
33. C.-H. Lee, H. Yoshida, Y. Miura, A. Fujii, and M. Ozaki, "Local liquid crystal alignment on patterned micrograting structures photofabricated by two photon excitation direct laser writing," *Appl. Phys. Lett.* **93**(17), 173509 (2008).

## 1. Introduction

Tunable-focus liquid crystal (LC) microlens array has become an essential optical component for image processing [1–12], beam steering [13–15], wavefront correction [16] and switchable 2D/3D displays [17–19]. A key to tune the focal length is to create parabolic phase profile by spatially controlling the LC director reorientations, such as introducing inhomogeneous electric field distribution or creating gradient pretilt angle alignment [20,21]. To do so, several approaches have been developed, including curved electrodes [22], patterned electrodes [23], polymer-stabilization [24], composite alignment [25], and composite lenses [26], just to name a few. As for the composite lenses, a reliable way of generating LC alignment on the polymer microlens array is crucial. Other than the traditional rubbing [26] and photoalignment methods [27], here we propose a new fabrication method to fulfil this goal with recently developed two-photon polymerization based direct-laser writing.

By utilizing the two-photon absorption property of certain photoresist, sub-micrometer sized pattern can be easily achieved through direct-laser writing [28,29]. This technique offers a new way for generating complex 2D/3D LC alignment to enable tunable photonic devices

[30–32] that are otherwise difficult to fabricate with conventional mechanical buffing methods.

In this paper, we apply direct-laser writing technique to polymerize a parabolic-shape microlens array on an indium tin oxide (ITO)-coated planar substrate. Such a parabolic-shape polymer surface not only generates the desired inhomogeneous electric field for a lens but also serves as LC alignment layer. By filling a LC mixture into the homogeneous alignment-like cell, the focal length of the microlens array is tunable by the applied voltage. In experiment, a  $16 \times 16$  microlens array with individual microlens size of  $120 \times 120 \mu\text{m}^2$  is fabricated. The voltage dependent focal length at different wavelengths is measured. The fabricated sample exhibits a conformal pretilt-angle, as evidenced by characterizing the phase profiles under different voltages. The focusing property at different wavelengths and the white-light imaging capability of the microlens array are also investigated. Through this work, it is evident that the direct-laser writing is a viable approach for simultaneously forming curvilinear-surface structure and patterning LC alignment on such a surface. It offers a new option for making other tunable LC photonic devices.

## 2. Methods

### 2.1 Two-photon polymerization based patterning

The polymerized microlens array with LC molecular alignment was fabricated using a commercial femtosecond laser lithography system (NanoScribe GmbH). A  $63 \times$ , 1.4 numerical aperture oil immersion objective (Zeiss) and IP-Dip (NanoScribe GmbH) photoresist, were used in dip-in mode. After dropping IP-Dip on a single-side ITO-coated glass substrate, the objective was directly immersed into the IP-Dip. A 2D galvanometer scanner was utilized to steer the focal point of a 780-nm pulsed laser in plane to expose the photoresist line-by-line. Grooves with 700-nm periodicity were established to provide anchoring force to LC molecules, where the anchoring energy is about  $5 \mu\text{J}/\text{m}^2$  [33]. After the writing, the sample was gently immersed into 1,2-Propanediol monomethyl ether acetate (PGMEA) solution for 20 min to remove the unexposed photoresist, and then it was placed in isopropyl alcohol for 5 min to remove PGMEA. Last, to evaporate the isopropyl alcohol, the sample was held at 20 cm above a 200 °C hot plate until all the droplets were completely evaporated.

### 2.2 LC cell formation

A single-side ITO-coated glass superstrate with rubbed alignment parallel to the direction of the polymerized nano-groove was adhered to the bottom substrate using NOA 81, together with sparsely distributed silica spacers to control the total cell gap ( $17.2 \mu\text{m}$ ). Once UV cured, the test cell was filled with a well-studied LC mixture E7 (Merck), whose refractive indices  $n_o = 1.52$  and  $n_e = 1.74$  at  $\lambda = 633 \text{ nm}$ , dielectric constants  $\epsilon_{\perp} = 5.1$  and  $\epsilon_{\parallel} = 19.5$  at 1 kHz driving frequency, and visco-elastic constant  $\gamma_1/K_{11} = 21.4 \text{ ms}/\mu\text{m}^2$  at room temperature. By contrast, the photoresist IP-DIP has  $n = 1.52$  and  $\epsilon = 4$  at 1-kHz driving frequency.

### 2.3 Characterization

The morphology of the structure was investigated by scanning electron microscopy (SEM) (Zeiss ULTRA-55 FEG SEM) at an accelerating voltage of 3.5 kV. The focal lengths were measured directly on an optical microscope (OLYMPUS BX51), and the images were collected using the same microscope with  $5 \times$  objective and an Infinity 2-2 camera. The test cell was driven with 1 kHz AC sine wave to reduce ion migration. All the reported voltages are root mean square values.

### 3. Results and discussion

Figure 1(a) depicts the schematic of the proposed tunable microlens array. The parabolic-shape microlens array is directly formed by two-photon polymerization to create inhomogeneous electric field distribution and homogeneous-like LC alignment, simultaneously. The laser-writing system divides the microlens array into many writing fields, with only one microlens in each writing field. Within one writing field, the microlens is divided into many layers and the photoresist is polymerized layer by layer. Each layer consists of 700-nm periodic grooves, exposed by the raster scan of the laser in the horizontal direction. After the exposure of one layer, the piezo-stage lifts the laser so that the laser can keep scanning in upper layers, until the individual microlens is finished. It is worth mentioning that between the microlenses and the substrate, there is a 500-nm thick uniform groove alignment covering the whole unit. This additional layer ensures that the area between the microlenses also has the groove alignment in the same direction, as depicted by the red arrow in Fig. 1(b). This layer is also generated by direct-laser writing, and it serves to minimize the random scattering out of the microlens area. However, it will shield the electric field and slightly increase the threshold voltage and the working voltage. Figure 2 illustrates the step-by-step fabrication process within one writing field, i.e. polymerization of a single microlens. In experiment, a  $16 \times 16$  microlens array is fabricated. The height of each parabolic-shape microlens is designed to be  $5 \mu\text{m}$ . Moreover, the periodicity of the microlens array is kept at  $120 \mu\text{m}$  and the diameter of each individual lens is  $120 \mu\text{m}$  as well, resulting in a fill factor of 78.5%. Another important aspect related to fabrication is the writing time. The laser lithography system took 20 seconds to polymerize a single microlens. Thus, it took about 90 minutes to finish the writing process for the  $16 \times 16$  microlens array sample.

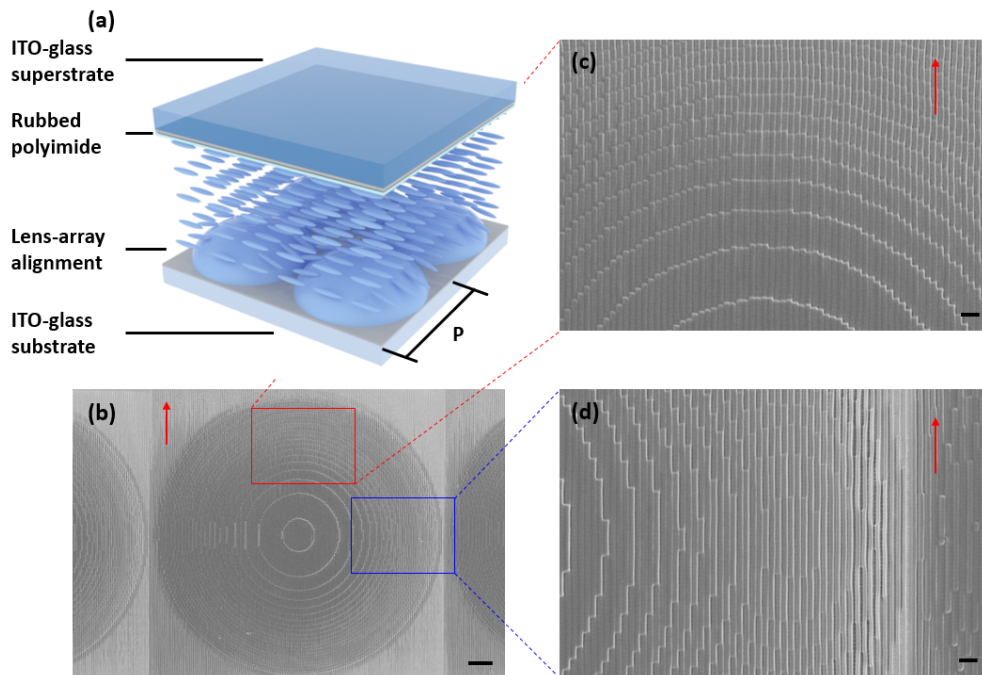


Fig. 1. (a) Schematic of the proposed structure, and (b-d) SEM images of a  $16 \times 16$  microlens array sample where each microlens is  $120 \times 120 \mu\text{m}^2$ . The series illustrate that the nano-groove directions at different parts, as highlighted by the red arrows, are the same. Scale bars:  $10 \mu\text{m}$  (b),  $2 \mu\text{m}$  (c), and  $2 \mu\text{m}$  (d).

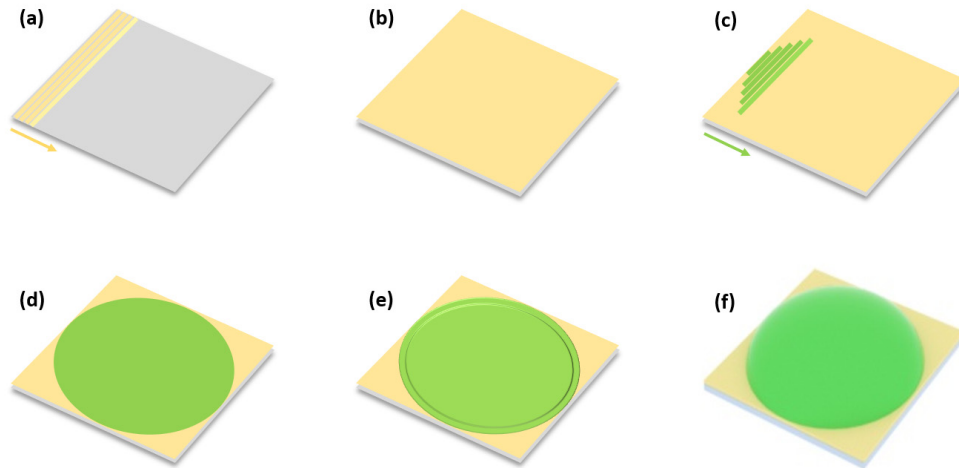


Fig. 2. Step-by-step fabrication process of a single microlens. After dropping IP-DIP photoresist on the ITO-coated substrate, a laser lithography system is applied to expose the photoresist line-by-line. (a) Line-by-line exposure to form a 500-nm thick uniform groove alignment covering the whole unit. The arrow shows the scanning direction. (b) Finish of the bottom uniform alignment layer. (c) Line-by-line exposure to form the very bottom layer of the microlens. The arrow depicts the scanning direction (d) Finish of the very bottom layer of the microlens. (e) After the exposure of the bottom layer of the microlens, the laser lithography system starts to expose the upper layer of the microlens in a layer-by-layer manner. (f) Finish of the single microlens. After the finish this writing field, the laser system will move to the next writing field and keep scanning until the whole structure is accomplished.

Figures 1(b)-1(d) show a portion of the surface profile of the exposed microlens array under SEM. As noticed, the polymerized microlenses are digitized, both in vertical direction and in the horizontal plane. The digitization in horizontal plane is required by the groove period and it can be diminished by reducing the groove period. On the other hand, the digitization in vertical direction is crucial for providing strong-enough anchoring force to the LC molecules. Compared to the digitization in the horizontal plane, the discreteness in vertical direction makes a higher impact to the microlens performance, because of the relatively large difference between the scales ( $120\text{-}\mu\text{m}$  radius versus  $5\text{-}\mu\text{m}$  height) but with similar digitization step in these two dimensions. In our design, the step in vertical direction is approximately 200 nm. Figure 3 shows the detail of the digitized surface profile in a cross-section view. We further studied the effect of introducing the discreteness into the microlenses by comparing the focal spot of the digitized microlens to that of an ideal microlens. To specify, here only a single microlens is considered rather than an array, and thin-lens approximation and Fresnel approximation are applied in our calculations for simplicity. Figure 4 depicts the cross-section of the intensity profiles at the focal plane in air. A slight (7.7%) decrease of the peak intensity, in comparison with the ideal case, is found at  $\lambda = 633\text{ nm}$ .



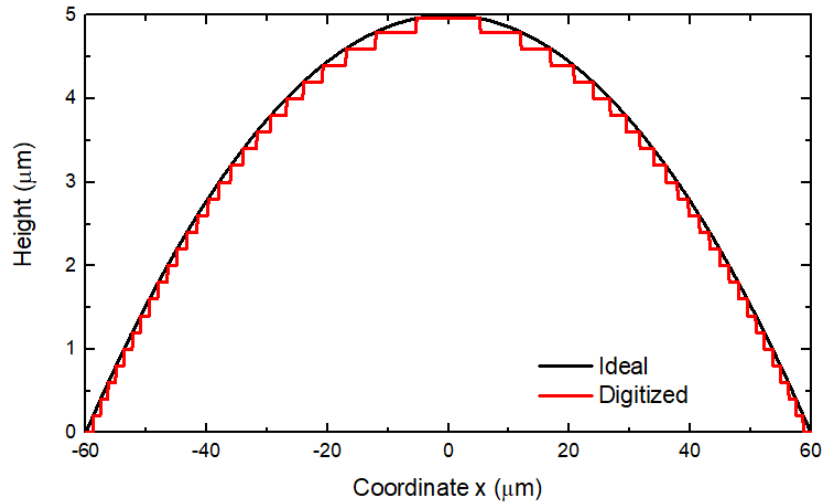


Fig. 3. Cross-section view of the microlens profiles. The black line denotes the ideal parabolic surface profile and the red line depicts the digitized surface profile.

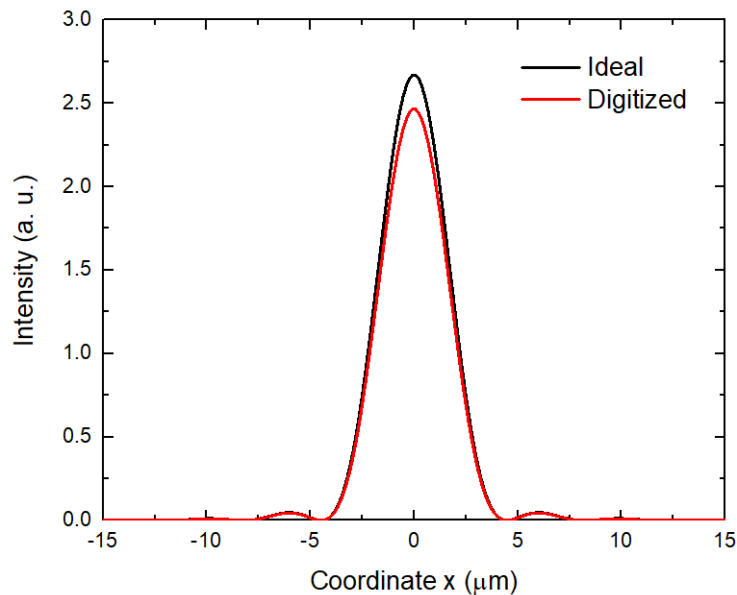


Fig. 4. Calculated cross-section of the focal spot for the two cases. The black line denotes the result of the ideal parabolic surface profile and the red line depicts the results of the digitized surface profile.  $\lambda = 633$  nm.

As mentioned earlier, the microlens array itself provides alignment along one direction. This can be seen from Figs. 1(b)-1(d), where different parts of the microlens have nano-grooves along the same direction. An important parameter here is the depth of the grooves, which turns out to be less than 100 nm. This ensures that even the period of the grooves is larger than the wavelength, diffraction effect arising from the grooves remains negligible. To further finish the cell, another top superstrate with rubbed homogeneous alignment along the direction of the nano-grooves is adhered to the bottom substrate. After filling with LC materials, the LC cell in total is akin to a homogeneous alignment cell, resulting in a bifocal

microlens array. We also inspected the haze of the assembled microlens array cell, and it is quite clear visually.

To measure the focal length of the microlens array under different voltages, we used an optical microscope with linearly polarized input light. After aligning the direction of the nano-grooves to the polarization of the input light, we measured the focal length through adjusting the height of the stage from a clear focal point to the bottom substrate. The focal length was directly read out from the scale of the microscope. Figure 5 depicts the voltage dependent focal length of the fabricated microlens array at three specified wavelengths. It is worth mentioning that the depth of focus of the microlens array is around 0.3 mm, leading to variations when measuring focal lengths. Our designed microlens is essentially a composite lens, consisting of a convex polymer lens and a concave LC lens. Without voltage, the composite microlens is concave since the extraordinary refractive index ( $n_e = 1.74$ ) of the LC material is larger than the refractive index of the photoresist ( $n = 1.52$ ). Above the threshold voltage ( $V_{th} \approx 1.5$  V), the focal length of the concave LC lens starts to increase, and the composite microlens finally becomes convex at around 1.8 V. For our test cell in the convex tuning range, a well-defined focus can be found from 1.8 V to 4.5 V, and the focal length has a minimum at around 2.6 V. This trend of focal length tuning is similar to that reported in [26] because of the similar lens configuration.

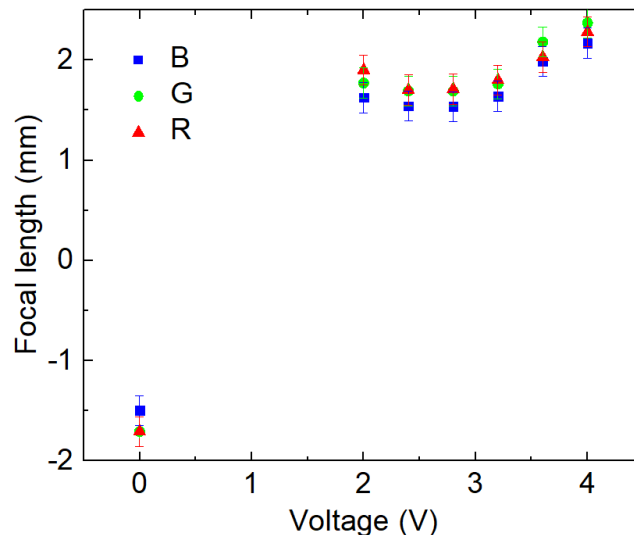


Fig. 5. Measured voltage dependent focal length of our fabricated microlens array at three specified wavelengths: R = 633 nm, G = 546 nm, and B = 450 nm.

Figure 6 shows the extracted phase profiles along  $x$  and  $y$  directions, as a function of applied voltages. To extract the phase profile of a single microlens in both  $x$  and  $y$  directions, polarized optical microscopy (POM) is applied where the direction of the nano-groove is at  $45^\circ$  to the crossed polarizers. All the phase profiles are directly extracted from the inset POM images, where a green interference color filter ( $\lambda \approx 546$  nm) is utilized to generate narrow-band light source. It can be seen that at 2 V, there is a plateau in the central part, along  $x$  direction. This is due to the increased voltage shielding as the polymer thickness increases. At this voltage, the central part of the LC molecules is still not responding to the applied field, leading to the plateau in the phase profile. Another noteworthy phenomenon of this microlens array can also be seen from Fig. 6. Without voltage, the phase profile of the microlens is perfectly centrosymmetric. In the presence of voltage, the sample has astigmatism-like aberration below 3.6 V, where the characteristic of the aberration resembles that in [26]. This phenomenon indicates that the polymer microlens produce a conformal pretilt angle. The

pretilt direction on the bottom substrate is parallel to that on the top superstrate on one side of the microlens, but anti-parallel to that on the top superstrate on the other side of the microlens. The asymmetry of the pretilt angle causes strong asymmetry of the LC morphology when the applied voltage is slightly above  $V_{th}$ . However, the asymmetry of the LC directors diminishes after further increasing the applied voltage. At 3.6 V, the astigmatism-like aberration is almost indiscernible. In our previous work [30,32], when using two-photon polymerization direct-laser writing technique to create planar alignment, no pretilt-angle effect was observed. Here we experimentally demonstrate that the pretilt angle can be generated by this technique, on curvilinear surfaces. Further studies may apply this technique to engineer the pretilt angles.

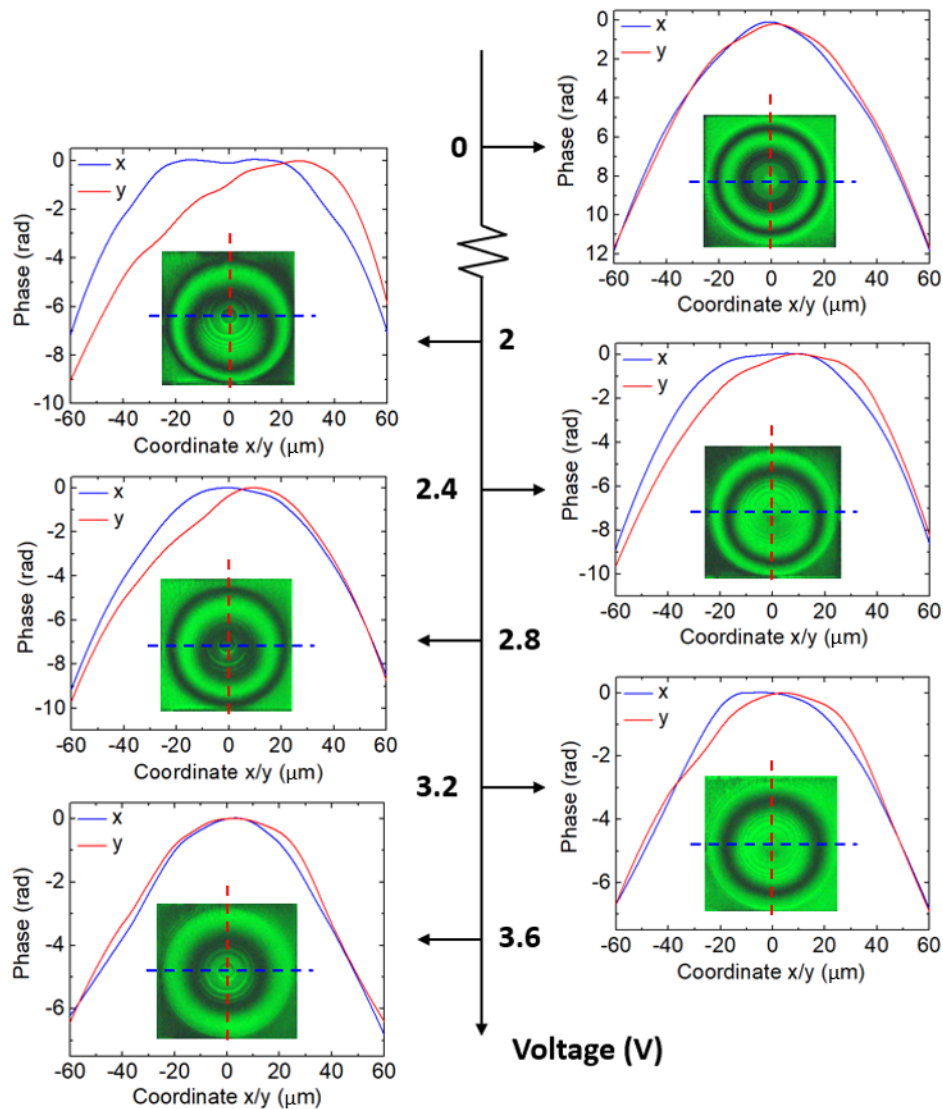


Fig. 6. Extracted phase profiles along  $x$  and  $y$  directions as a function of applied voltage. Inset is the polarized optical microscopy image of a single microlens. The blue and red dashed lines indicate the  $x$  and  $y$  directions, respectively.

Figure 7 summarizes the focusing property of the microlens array at different wavelengths as a function of applied voltage. For each color, the intensity of the light source is the same.



As the applied voltage increases, a noticeable drop of focusing power can be seen. But for all the cases in Fig. 7, the designed microlens array can generate well-defined focal points, even though astigmatism-like aberration exists in some cases. As can be noticed, the background is not completely dark. This is caused by several factors, such as the not 100% fill factor, the deviation from ideal phase profile of the microlens, and the diffraction effect of the array.

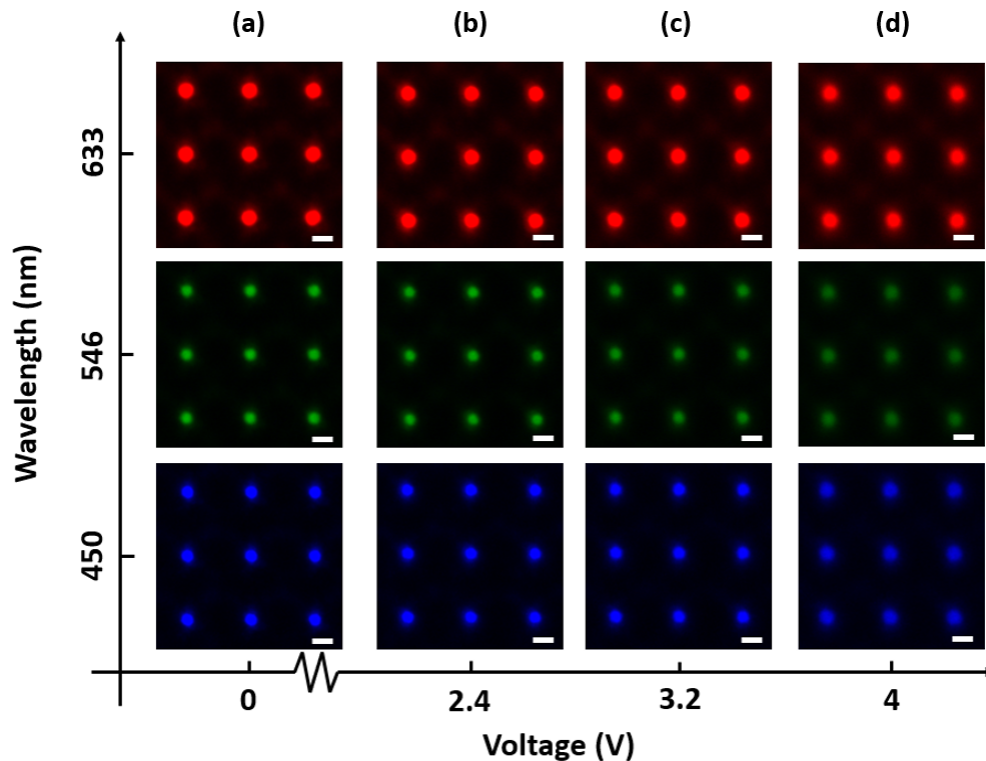


Fig. 7. The focusing property of the fabricated sample at different wavelengths as a function of applied voltages, which are 0 V for (a), 2.4 V for (b), 3.2 V for (c) and 4 V for (d). The images are captured under the microscope where different color filters are selected to choose the desired wavelength of the incident light. Scale bar: 20  $\mu\text{m}$  for all.

As a microlens, imaging capability is another important aspect. Figure 8 shows the white-light (halogen) microscopic images of the imaging targets and the images formed by the microlens array under different applied voltages where the targets are 4.4 mm away from the bottom substrate of the sample. For different applied voltages, the distance between the cell and the camera is adjusted such that the images are captured at the image plane. As noticed in Fig. 8, without voltage, the images are virtual and erect in that the microlens array is concave. On the other hand, the images are real and inverted in the other cases since the microlens array is convex. In our experiment, three-bar target and four-dot target are chosen to test the resolving ability of the microlens array. It turns out that the three-bar target with 57.0 lp/mm resolution can be resolved and the four-dot target can also be separated well. We also employ the 'UCF' letters to demonstrate the imaging of a non-centrosymmetric pattern, which shows clear images in both concave and convex cases.

From the above characterizations, the composite-lens adaptive microlens array is turned out to be well-functioning. By using the microlens array as an example, we show that the use of two-photon polymerization direct-laser writing to create curvilinear-surface structure with LC alignment is feasible. Furthermore, by exposing the photoresist and forming the groove in different directions in space, arbitrary patterning on curvilinear surfaces is possible.

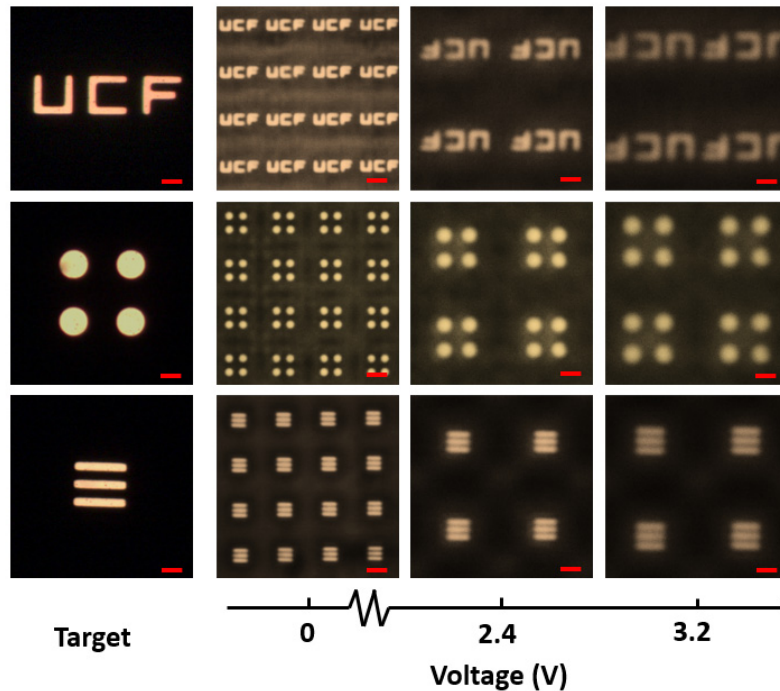


Fig. 8. White-light imaging capability for different targets as a function of applied voltage. From top to bottom: 'UCF' letters, four-dot target and three-bar target. Scale bar:  $20\ \mu\text{m}$  for all.

#### 4. Conclusion

A LC-based tunable  $16\times 16$  microlens array with individual microlens size  $120\times 120\ \mu\text{m}^2$  is fabricated and characterized. The key parabolic-shape structure, for creating inhomogeneous electric field distribution and homogeneous-like LC alignment, is directly formed through two-photon polymerization direct-laser writing. After finishing the test cell, the focal lengths at different wavelengths as a function of voltage are measured. The fabricated sample shows pretilt-angle effect on LC directors, which has not been discovered in our previous work. We also evaluate the focusing property at different wavelengths and the white-light imaging capability of the sample. Using the microlens array as an example, we show that the use of two-photon polymerization direct-laser writing to create curvilinear-surface structure with LC alignment is feasible. It opens a new door for arbitrary patterning on curvilinear surfaces. In addition to adaptive lenses, the direct-laser writing method will enable other practical tunable photonic devices.

#### Funding

Intel Corporation and National Science Foundation (NSF) (ECCS-1509729).

#### Acknowledgments

We are indebted to Yuge Huang and Dr. Hongwen Ren for helpful discussion.